Electron Spin Resonance Studies of Cu^{2+} Doped in Single Crystals of Cytosine Monohydrate

Kazumi Toriyama and Machio Iwasaki*

Contribution from Government Industrial Research Institute, Nagoya Hirate, Kita, Nagoya, Japan. *Received February 17, 1975*

Abstract: Electron spin resonance (ESR) studies were made on Cu^{2+} interstitially doped in single crystals of cytosine monohydrate. It was found that Cu^{2+} ions in this crystal form distorted square planar complexes with cytosine molecules. This is the first ESR evidence that interstitially doped Cu^{2+} can complex with nucleic acid bases in the crystalline state. ESR spectra showed a ligand superhyperfine structure arising from a strongly coupled nitrogen. The spin Hamiltonian parameters such as **g**, $\mathbf{A}^{Cu}$, and $\mathbf{A}^{N}$ tensors were determined together with the quadrupole interaction parameter Q. From these magnetic tensors, the probable Cu^{2+} binding site was suggested to be the plane made by the two adjacent cytosine molecules linked by the two intermolecular hydrogen bonds, which are quite similar to those in the C-G and A-T(U) pairs in the double helix of DNA and RNA.

ESR studies of Cu^{2+} ions doped in single crystals of amino acids have been reported by many workers.[1] It has been found that the Cu^{2+} ions interstitially doped in the crystals form square planar complexes with host molecules. However, there seems to be no report on ESR of copper(II) complexes of nucleic acid bases. On the other hand, it has been suggested that copper ions and some other divalent metal ions form complexes with DNA bases. Since Cu ions influence the stability of the double helix of DNA,[2] interaction between DNA and Cu ions has received considerable attention.[3] However, binding sites have not been well elucidated.

Recently we have accidentally found that crystals of commercially obtained cytosine monohydrate contain Cu^{2+} ions as an impurity. It has been further found that Cu^{2+} ions can be doped in single crystals of pure cytosine monohydrate when they are grown from aqueous solutions containing copper nitrate and that the ESR spectra of Cu^{2+} are identical with those of the above-mentioned impure cytosine. It is of considerable interest to study the copper binding sites of the crystal of cytosine in relation to the complex formation of Cu^{2+} with nucleic acid constituents. This paper describes the spin Hamiltonian parameters of Cu^{2+} in cytosine monohydrate crystals and its probable binding sites.

Experimental Section

Single crystals of Cu^{2+}-doped cytosine monohydrate were grown from aqueous solutions containing a 10^{-3} mol fraction of copper nitrate by slow evaporation at room temperature. The Cu^{2+}-doped crystals in which NH and water protons are deuterated were also grown from the heavy water solutions. Because of better resolution of the ESR spectra, the deuterated crystals were mainly used for the spectral analyses. The Cu^{2+}-doped crystals exhibited the same crystal habits as those of the pure cytosine monohydrate, which is known to be monoclinic with a space group of $P2_1/c$.[4] From the angular variation of the ESR spectra of radiation induced radicals originating from host molecules, it has been confirmed that the Cu^{2+}-doped crystals have the same crystal structure as those of pure cytosine monohydrate except for the slight deformation in the local structure around Cu^{2+}.

The ESR spectra of Cu^{2+} ions were measured with a Varian E-12 spectrometer operated at X-band with 100 KHz and 35 Hz double modulations. The spectra obtained at room temperature were essentially the same as those obtained at 77 K so that the analyses were made for the spectra obtained at room temperature. The experimental coordinate system used is a*, b, and c, in which $\mathbf{a}^* = \mathbf{b} \times \mathbf{c}$. The atomic numbering system employed in this article is given in Figure 1.

Analyses

The spin Hamiltonian of our system is given by the following equation if the superhyperfine interaction with ligand nitrogen is omitted:

$$\mathcal{H} = \beta H\tilde{\mathbf{S}}\cdot\mathbf{g}\cdot\mathbf{h} + \tilde{\mathbf{I}}\cdot\mathbf{A}\cdot\mathbf{S} + \tilde{\mathbf{I}}\cdot\mathbf{P}\cdot\mathbf{I} - g_n\beta_n H\tilde{\mathbf{I}}\cdot\mathbf{h} \quad (1)$$

where **h** is the unit vector along the external magnetic field and other symbols refer to the usual conventions. Within a limit of high field approximation, a general solution to the second order has been derived for the Hamiltonian in an arbitrary coordinate system without making the assumption that the **g**, **A**, and **P** tensors are coaxial. The only restriction is that the effective hyperfine Hamiltonian including the nuclear Zeeman term be much greater than the quadrupole term. The results are given in ref 5. Using this general solution with an additional assumption that the nuclear Zeeman term is much smaller than the hyperfine term, the resonance fields and the relative intensities of the ESR absorptions of Cu^{2+} ($S = \frac{1}{2}$, $I = \frac{3}{2}$) are given by the following equations:

$\Delta M_I = 0$ transitions

$$H(\pm\tfrac{3}{2}) = (g_0/g)\left[H_0 \mp \frac{3}{2}K - \frac{A_{3/2}}{8(H_0 \mp 3K/2)} \mp 3P_{3/2}/K\right] \quad (2)$$

$$H(\pm\tfrac{1}{2}) = (g_0/g)\left[H_0 \mp \frac{1}{2}K - \frac{A_{1/2}}{8(H_0 \mp K/2)} \mp 3P_{1/2}/K\right] \quad (3)$$

$\Delta M_I = \pm 1$ transitions

$$H\left\{\left(\frac{1}{2}, \pm\frac{3}{2}\right) \leftrightarrow \left(-\frac{1}{2}, \pm\frac{1}{2}\right)\right\} = (g_0/g) \times \left[H_0 \mp K - 3(\tilde{\mathbf{k}}\cdot\mathbf{P}\cdot\mathbf{k}) \pm H_n - \frac{A_\mp}{H_0 \mp K} \mp 3P_2/2K\right] \quad (4)$$

$$H\left\{\left(\frac{1}{2}, \pm\frac{1}{2}\right) \leftrightarrow \left(-\frac{1}{2}, \pm\frac{3}{2}\right)\right\} = (g_0/g) \times \left[H_0 \mp K + 3(\tilde{\mathbf{k}}\cdot\mathbf{P}\cdot\mathbf{k}) \mp H_n - \frac{A_\pm}{H_0 \mp K} \mp 3P_2/2K\right] \quad (5)$$

$$I(\Delta M_I = \pm 1) = 48P_1/K^2 \quad (6)$$

$\Delta M_I = \pm 2$ transitions

$$H\left\{\left(\frac{1}{2}, \pm\frac{3}{2}\right) \leftrightarrow \left(-\frac{1}{2}, \mp\frac{1}{2}\right)\right\} = (g_0/g)\left[H_0 \mp \frac{1}{2}K -$$

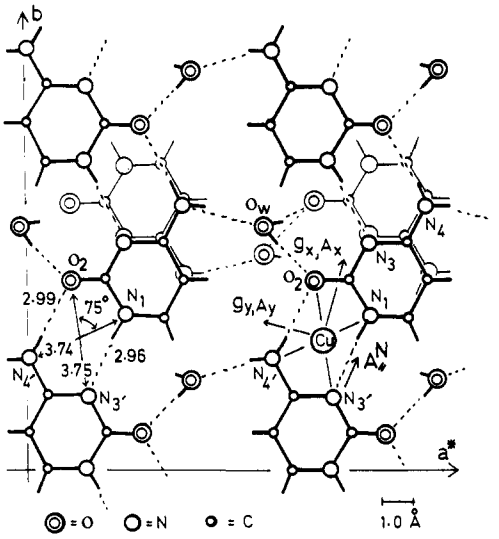

Figure 1. Crystal structure and the atomic numbering system for cytosine monohydrate. A part of the molecules lying in the lower layer are shown by the thin lines. The proposed Cu^{2+} site in this crystal is also shown together with the principal directions of the observed **g**, $\mathbf{A}^{Cu}$, and $\mathbf{A}^{N}$ tensors.

$$3(\tilde{\mathbf{k}}\cdot\mathbf{P}\cdot\mathbf{k}) \pm 2H_n - \frac{A_{\mp}'}{H_0 \mp K/2} \mp 12P_1/K \Big] \quad (7)$$

$$H\left\{\left(\frac{1}{2}, \pm\frac{1}{2}\right) \leftrightarrow \left(-\frac{1}{2}, \mp\frac{3}{2}\right)\right\} = (g_0/g)\left[H_0 \pm \frac{1}{2}K + 3(\tilde{\mathbf{k}}\cdot\mathbf{P}\cdot\mathbf{k}) \pm 2H_n - \frac{A_{\mp}'}{H_0 \pm K/2} \pm 12P_1/K\right] \quad (8)$$

$$I(\Delta M_I = \pm 2) = 3P_2/K^2 \quad (9)$$

where **k** is the unit vector along the nuclear quantization axis and

$$A_{3/2} = 3[Tr\mathbf{A}^2 + 2(\tilde{\mathbf{k}}\cdot\mathbf{A}^2\cdot\mathbf{k}) - 3K^2] \quad (10)$$

$$A_{1/2} = 7Tr\mathbf{A}^2 - 6(\tilde{\mathbf{k}}\cdot\mathbf{A}^2\cdot\mathbf{k}) - K^2 \quad (11)$$

$$P_{3/2} = Tr\mathbf{P}^2 + 2(\tilde{\mathbf{k}}\cdot\mathbf{P}^2\cdot\mathbf{k}) - 7(\tilde{\mathbf{k}}\cdot\mathbf{P}\cdot\mathbf{k})^2/2 \quad (12)$$

$$P_{1/2} = Tr\mathbf{P}^2 - 6(\tilde{\mathbf{k}}\cdot\mathbf{P}^2\cdot\mathbf{k}) + 9(\tilde{\mathbf{k}}\cdot\mathbf{P}\cdot\mathbf{k})^2/2 \quad (13)$$

$$A_{\pm} = \frac{5}{8}(Tr\mathbf{A}^2 - K^2) \pm \det\mathbf{A}/4K \quad (14)$$

$$A_{\pm}' = \frac{5}{8}(Tr\mathbf{A}^2 - K^2) \pm \det\mathbf{A}/2K \quad (15)$$

$$P_1 = (\tilde{\mathbf{k}}\cdot\mathbf{P}^2\cdot\mathbf{k}) - (\tilde{\mathbf{k}}\cdot\mathbf{P}\cdot\mathbf{k})^2 \quad (16)$$

$$P_2 = 2Tr\mathbf{P}^2 - 4(\tilde{\mathbf{k}}\cdot\mathbf{P}^2\cdot\mathbf{k}) + (\tilde{\mathbf{k}}\cdot\mathbf{P}\cdot\mathbf{k})^2 \quad (17)$$

$$\mathbf{k} = \mathbf{A}\cdot\mathbf{g}\cdot\mathbf{h}/gK \quad (18)$$

$$K = (\tilde{\mathbf{h}}\cdot\tilde{\mathbf{g}}\cdot\mathbf{A}^2\cdot\mathbf{g}\cdot\mathbf{h})^{1/2}/g \quad (19)$$

$$g = (\tilde{\mathbf{h}}\cdot\mathbf{g}^2\cdot\mathbf{h})^{1/2} \quad (20)$$

$$H_0 = h\nu/g_0\beta \quad (21)$$

$$H_n = (g_n\beta_n H/g_0\beta) \times (\tilde{\mathbf{h}}\cdot\mathbf{g}\cdot\mathbf{A}\cdot\mathbf{h})/gK \quad (22)$$

The spin Hamiltonian parameters were determined by the least-squares method so as to minimize $\Sigma(H_{obsd} - H_{calcd})^2$ for the allowed four transitions using eq 2 and 3. The starting parameters required for the nonlinear least-squares fitting procedure were obtained by the conventional method. In the present case, the quadrupole interaction parameter Q ($\equiv 2P_z/3$) is relatively small, and the reliable results were not obtained from the allowed transitions. Therefore, the $\Delta M_I = \pm 1$ forbidden transitions, which were observed in some limited crystalline orientations, were used to estimate the Q values.

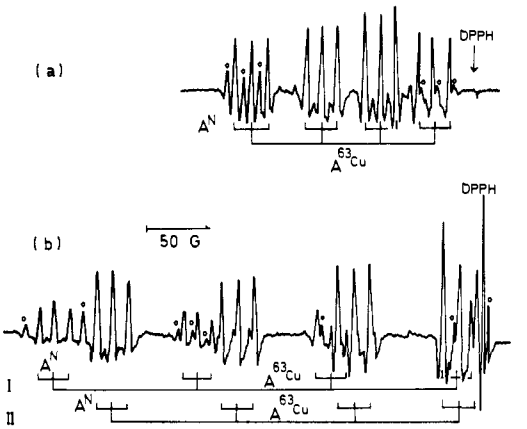

Figure 2. ESR spectra of Cu^{2+} doped in deuterated crystals of cytosine monohydrate. The spectra were taken at room temperature with an X-band spectrometer with the magnetic field applied along (a) −73° from the c axis in the ca* plane, and (b) 10° from the a^* axis in the a^*b plane. The lines marked with circles are the hyperfine lines arising from ^{65}Cu.

The superhyperfine coupling tensor of ^{14}N was determined by the conventional method using the least-squares technique.

Results

Shown in Figure 2 are the ESR spectra of Cu^{2+} in deuterated crystals. Spectra (a) and (b) were measured with the magnetic field applied along −73° from the c axis in the ca^* plane and 10° from the a^* axis in the a^*b plane, respectively. Signals marked I and II in Figure 2b are due to the magnetically nonequivalent two sites. The four-line hyperfine structure of $^{63}Cu^{2+}$ further splits into three lines with equal intensity. Although the analyses were not made, the satellite lines arising from ^{65}Cu are also seen in Figure 2. The superhyperfine structure which is attributable to the coupling with ^{14}N was always three lines in any crystalline orientation. This indicates that only one ligand nitrogen atom interacts strongly with Cu^{2+}. Since the deuterium substitution did not alter the superhyperfine structure, there is no proton which interacts strongly with Cu^{2+}.

The angular variations of the four hyperfine lines are shown in Figures 3-5. The splitting of the spectra arising from the magnetically nonequivalent two sites exhibited monoclinic symmetry. This indicates that the copper ions in the crystal occupy only a single specific position and preserve the symmetry of the host crystal. However, as will be discussed later, the magnetically nonequivalent two coordination planes of Cu^{2+} are slightly distorted from those expected from the structure of pure crystals. This distorsion results in the observed site splitting being larger than that expected. It is of considerable interest to note that the ESR intensities of the two sites are not equal as shown in Figure 2b. This may be due to a sort of epitaxial growth of the Cu-doped crystals. The distortion arising from interstitial copper ions does possess monoclinic symmetry and should lead to equal populations of the two sites. However, if the distortion brought from a copper ion influences the crystal growth in which successive copper ions in the same site are favorable, the nonequivalent population of the two sites may result.

The principal values and their directions of the **g**, $\mathbf{A}^{Cu}$, and $\mathbf{A}^{N}$ tensors are given in Table I together with the Q values. The solid and broken lines in Figures 3-5 are the calculated angular variations from these values. Although

Table I. Spin Hamiltonian Parameters for Cu^{2+} Centers in the Single Crystals of Cytosine Monohydrate. The Principal Elements of $\mathbf{A}^{Cu}$ and $\mathbf{A}^{N}$ Tensors and Q are in Units of 10^{-4} cm^{-1}

	Principal values	Direction cosines[b] a^*	b	c	
g_x	$2.053_8 \pm 0.005$	0.246	∓0.960	0.135	23° with (3)
g_y	$2.057_5 \pm 0.005$	0.841	±0.142	−0.522	30° with (4)
g_z	$2.253_9 \pm 0.005$	0.482	±0.242	0.842	17° with (5)
$A_x{}^{63}Cu$	-9.6 ± 5.0[a]	0.259	∓0.960	0.103	2° with g_x
$A_y{}^{63}Cu$	-17.5 ± 5.0[a]	0.833	±0.168	−0.528	<1° with g_y
$A_z{}^{63}Cu$	-182.0 ± 2.0	0.490	±0.223	0.843	<1° with g_z
$Q(\equiv 2P_z/3)$	5 ± 2				
$A^{N\parallel}$	14.5 ± 0.5	0.396	∓0.910	−0.121	1° with (2)
$A^{N\perp}$	10.7 ± 0.5		$\perp$ to $A^{N\parallel}$		
(1) $N_4'-H\cdots O_2$		0.419	∓0.859	−0.295	
(2) $N_3'\cdots H-N_1$		0.426	∓0.886	−0.261	
(3) $N_3'\cdots O_2$		−0.139	∓0.990	0.008	
(4) $N_1\cdots N_4'$		0.810	∓0.377	−0.449	
(5) Normal to (3) and (4)		0.464	∓0.058	0.884	

[a] Signs of $A_x{}^{Cu}$ and $A_y{}^{Cu}$ of ^{63}Cu were assumed to be negative from the relation required for the deviation from axial symmetry of g and hyperfine tensors. [b] The estimated error for the principal axis is ±3° for g_z and A_z, and ±5° for $A^{N\parallel}$. The x and y principal directions are less reliable.

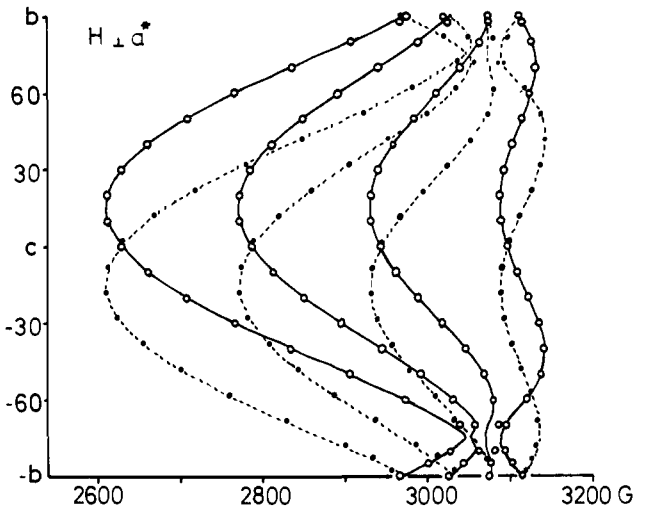

Figure 3. The angular variation of the four hyperfine lines of Cu^{2+} in the bc plane. The open and filled circles indicate the observed line positions of the two magnetically unequivalent sites. The solid and dotted lines are the calculated angular variations from the spin Hamiltonian parameters listed in Table II.

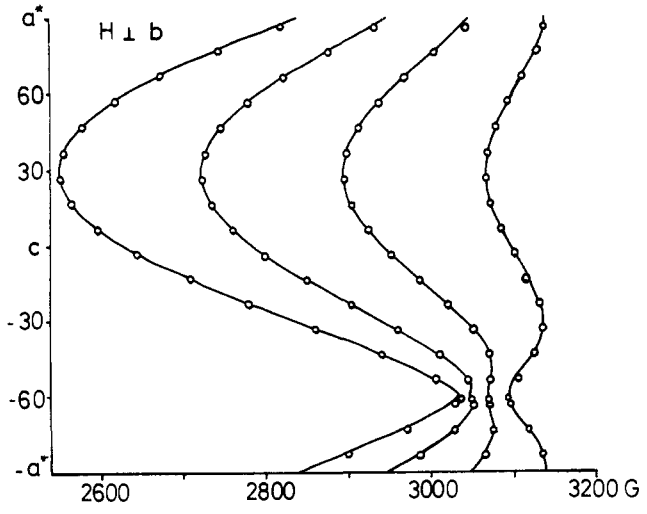

Figure 4. The angular variation of the four hyperfine lines of Cu^{2+} in the ca^* plane. The other remarks are the same as those given in Figure 3.

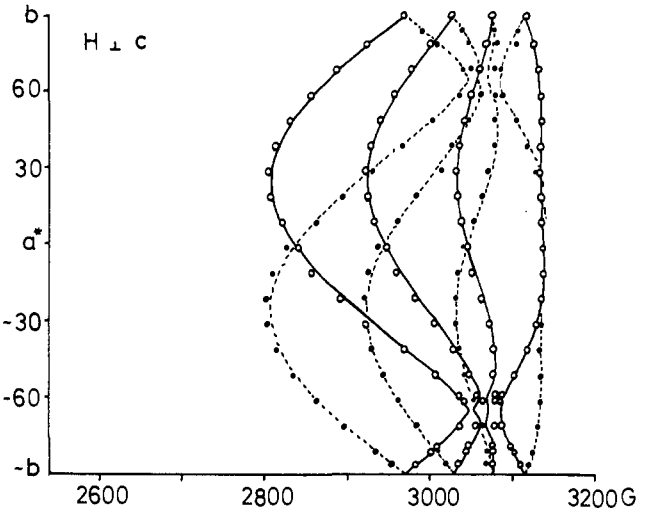

Figure 5. The angular variation of the four hyperfine lines of Cu^{2+} in the a^*b plane. The other remarks are the same as those given in Figure 3.

excellent agreement was obtained for most crystalline orientations, the calculated line positions showed considerable deviations from the observed ones in some directions which are close to the smallest principal element of the $\mathbf{A}^{Cu}$ tensor. This is due to the failure of the second-order perturbation approximation for the directions in which the hyperfine coupling is comparable with the quadrupole interaction. Therefore, the exact solutions were obtained for these directions by numerically diagonalizing the 8 × 8 spin Hamiltonian matrix. The results suggest that the value of $|A_x|$ is about 5×10^{-4} cm^{-1} which is slightly smaller than 9.6×10^{-4} cm^{-1} obtained from the least-squares method based on the second-order solutions. However, the complete analyses of the hyperfine patterns were not feasible because of the complication of the hyperfine multiplet arising from the ^{14}N coupling. Although the following discussion will be made based on the results obtained from the least-squares method, the essential feature of the conclusion may not be affected by the slight ambiguity in the value of $|A_x|$.

Discussion

Site of Cu^{2+}. The observed $\mathbf{g}$ and $\mathbf{A}^{Cu}$ tensors are nearly coaxial (within 1-2°) and approximately axially symmetric

Table II. Bonding Parameters and Spin Density Distribution in Ligands for Cu^{2+} Centers in Cytosine Monohydrate

p (cm^{-1})	κ	α_1^2	$\alpha_1'^2$	S value (assumed)	Observed spin densities $\rho(N_3')_{2s}$	$\rho(N_3')_{2p}$	$\Sigma\rho(N_3')$	$\rho(N_1)+\rho(N_4')^c$	$a^{N_1}, a^{N_4'}$ ($\times 10^{-4}$ cm^{-1})^d
0.036 (assumed)	0.38[a]	0.84[a]	0.24	0.091	0.02	0.08	0.10	0.04	3.0
			0.23	0.080				0.03	2.2
			0.22	0.070				0.02	1.5
			0.21	0.060				0.01	0.7
			0.20	0.050				0.00	0.0

[a] Obtained from the observed g and A^{Cu} tensor elements, assuming -0.002, -0.002, and -0.02 for δ_x, δ_y, δ_z, respectively. [b] $a_{2s}^N = 514 \times 10^{-4}$ cm^{-1} for $\rho(N)_{2s} = 1$ and $B_\perp^N = -16 \times 10^{-4}$ cm^{-1} for $\rho(N)_{2p} = 1$ were used. [c] Assuming $\alpha_1'^2 = \rho(N_3') + \rho(N_1) + \rho(N_4') + \rho(O_2)$ and $\rho(N_3') = \rho(O_2)$, the values in this column are obtained from the relation $\rho(N_1) + \rho(N_4') = \alpha_1'^2 - 2\Sigma\rho(N_3')$. [d] The sp^2 hybridization were assumed.

with the relations $g_z \gg g_x \simeq g_y$ and $|A_z| \gg |A_x| \simeq |A_y|$. These features are characteristic of Cu^{2+} in square planar complexes in which the unpaired electron occupies mainly the $d_{x^2-y^2}$ orbital of a copper atom. The z axis, that is, the normal to the coordination plane, was found to be approximately perpendicular to the plane formed by the two neighboring cytosine molecules which are linked by the two hydrogen bridges $N_3'\cdots H\text{-}N_1$ and $N_4'\text{-}H\cdots O_2$ (see Figure 1). The A^{N_1} axis, which is to be parallel to the ligand nitrogen sp^n hybrid orbital, was found to be nearly parallel to the $N_3'\cdots H\text{-}N_1$ and $N_4'\text{-}H\cdots O_2$ hydrogen bond directions. Therefore, the coordination plane of Cu^{2+} in the crystal is assigned to $N_3'N_1O_2N_4'$. There are two coordination planes which are related by monoclinic symmetry. The two planes in the pure crystal are nearly parallel so that if the Cu-doped crystal has the same structure, the site splitting observed with the magnetic field in the bc plane should be very small. The observed large site splitting indicates that the coordination plane in the Cu-doped crystal deviates about 17° from that in the pure crystal. This distortion is considered to be brought from the interstitial copper ion complexing with the two cytosine molecules. However, since the precise geometry of the coordination plane in the Cu-doped crystal is not known, the following discussion will be made based on the geometry in the pure crystal.

The $N_3'\text{-}O_2$ and $N_1\text{-}N_4'$ distances in the host crystal are 3.75 and 3.74 Å, respectively, which are approximately two times the Cu-N and Cu-O bond distances (~1.9 Å). The angle made by the $N_3'\text{-}O_2$ and $N_1\text{-}N_4'$ vectors is 75°. The observed x and y principal axes of the **g** tensor are portrayed in the crystal structure shown in Figure 1. The x axis makes an angle of 23° with the $N_3'\text{-}O_2$ vector and the y axis of 30° with the $N_1\text{-}N_4'$ vector.

Since no appreciable coupling of protons was observed, the two hydrogen bonded protons are supposedly replaced by Cu^{2+} because of charge compensation. As a result, the in-plane lone pair electron orbitals of the three ligand nitrogen atoms are considered to direct along the $N_3'\text{-}N_1$ and the $N_4'\text{-}O_2$ vectors, which are approximately parallel to each other. This situation makes it difficult to identify which ligand nitrogen atom is responsible for the observed superhyperfine coupling. However, from the following two reasons, N_3' is likely the origin of the observed coupling: (1) if the ligand nitrogen atoms other than N_3' are responsible, both N_1 and N_4' would give nearly the same coupling because of their symmetrical location to the $d_{x^2-y^2}$ orbital of Cu^{2+}; (2) since the four ligand atoms form a rectangular coordination plane in which N_1 and N_4' are more closely situated in the nodal plane of the copper $d_{x^2-y^2}$ orbital, the lone pair orbital of N_3' more favorably overlaps with the $d_{x^2-y^2}$ oribital giving a large superhyperfine coupling. Thus, it may be expected that $a^{N_3'} \gg a^{N_1} \approx a^{N_4'}$.

To estimate the unpaired electron spin distribution in the ligand atoms, the bonding parameters have been calculated for our copper complex. Assuming that the ground orbital of Cu^{2+} is $d_{x^2-y^2}$ which is mixing with $d_{3z^2-r^2}$, the molecular orbitals for the d^9 positive hole are given by[6,7]

$$\Psi_{x^2-y^2} = \alpha_1(\cos\theta d_{x^2-y^2} + \sin\theta d_{z^2}) - \alpha_1'\phi_{x^2-y^2} \quad (23)$$

$$\Psi_{xy} = \alpha_2 d_{xy} - \alpha_2'\phi_{xy} \quad (24)$$

$$\Psi_{z^2} = -\sin\theta d_{x^2-y^2} + \cos\theta d_{z^2} \quad (25)$$

$$\Psi_{yz} = \alpha_3 d_{yz} - \alpha_3'\phi_{yz} \quad (26)$$

$$\Psi_{zx} = \alpha_4 d_{zx} - \alpha_4'\phi_{zx} \quad (27)$$

where ϕ's denote the ligand molecular orbitals which give the nonvanishing overlap with the copper d orbitals. In this approximation, the orbital contribution arising from the spin-orbit coupling gives the following relations to the principal elements of the $\mathbf{A}^{Cu}$ tensor:

$$A_x/p = (-\kappa + \tfrac{2}{7})\alpha_1^2 + \Delta g_x - (\tfrac{3}{14})\Delta g_y \quad (28)$$

$$A_y/p = (-\kappa + \tfrac{2}{7})\alpha_1^2 + \Delta g_y - (\tfrac{3}{14})\Delta g_x \quad (29)$$

$$A_z/p = (-\kappa - \tfrac{4}{7})\alpha_1^2 + \Delta g_z + (\tfrac{3}{14})(\Delta g_x + \Delta g_y) \quad (30)$$

with

$$\Delta g_i = g_i - g_f - \delta_i \quad (31)$$

$$p = 2\gamma\beta_e\beta_n\langle r^{-3}\rangle \quad (32)$$

$$p\kappa = (\tfrac{16}{3})\pi\gamma\beta_e\beta_n\delta(r) \quad (33)$$

where δ_i is the minor contributions arising from the ligand molecular orbitals and from the slight mixing of d_{z^2} with $d_{x^2-y^2}$. Assuming[6b,7] $p = 0.036$ cm^{-1} and $\delta_i = -0.002$ to -0.02, α_1^2 and κ are obtained to be 0.84 and 0.38, respectively, from the observed **g** and $\mathbf{A}^{Cu}$ tensor elements. In this evaluation, the signs of A_x and A_y are assumed to be negative. The other sign combinations seem unlikely because they do not give appropriate values for κ and do not lead to the reasonable relation required for the deviation from axial symmetry of the **g** and $\mathbf{A}^{Cu}$ tensors.

To estimate the ligand MO coefficient α_1' from the normalization condition, the value of the ground-state overlap integral S is to be assumed. Therefore, $\alpha_1'^2$ obtained from a number of assumed values for S is given in Table II. The maximum S value, 0.091, is based on $S_{nitrogen} = 0.093$ and $S_{oxygen} = 0.076$, which are given by Kivelson and Neiman for the regular square planar complexes.[6b] In our distorted square complexes, S would be considerably smaller than these values.

On the other hand, from the observed $\mathbf{A}^N$ tensor the spin density on the N_3' atom was estimated to be $\rho_{2s}^N = 0.02$ and $\rho_{2p}^N = 0.08$, the net spin density on N_3' being 0.1. From the symmetry consideration, the spin density on the O_2 atom would be approximately the same as that on the N_3' atom. Therefore, by subtracting 0.2 (=0.1 × 1) from the value of $\alpha_1'^2$, the spin densities on N_1 and N_4' were es-

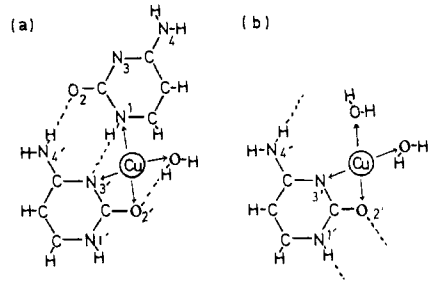

Figure 6. The alternative Cu^{2+} sites which might be possible: (a) if the large displacement of the water molecule is resulted from coordination with Cu^{2+}, (b) if one of the cytosine molecules is replaced by an water molecule.

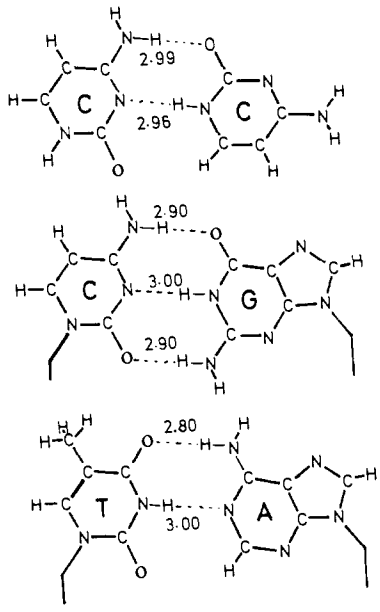

Figure 7. Hydrogen bonded plane formed between the two adjacent molecules in cytosine monohydrate and those formed in cytosine-guanine and adenine-thymine(uracil) pairs in the double helices of DNA and RNA.

timated and are given in Table II. As is seen, $\rho(N_1)$ and $\rho(N_4')$ are at most 0.021 which is considerably smaller than $\Sigma\rho(N_3') = 0.1$. If the overlap integral S is considerably smaller than 0.091 as is mentioned above, no resolvable superhyperfine couplings of N_1 and N_4' would be observed. Missing of ligand nitrogen superhyperfine couplings in such distorted planar complexes has been reported for Cu^{2+}-doped alanine by Fujimoto and Janecka[1d] and by Wilkinson and Miyagawa.[1e]

We have carefully examined other possible sites of Cu^{2+} in the cytosine monohydrate crystal. However, there is no other coordination plane which is consistent with the observed magnetic tensors, unless large displacements of the cytosine and water molecules are assumed in the doped crystal lattice. Although it is less probable, the site shown in Figure 6a might be possible, if the water molecule can largely move in the lattice forming coordination with Cu^{2+}. Similarly, if one assumes the cytosine vacancy which is filled by one water molecule forming coordination with Cu^{2+} as shown in Figure 6b, complexing with one nitrogen and three oxygen atoms might be possible, resulting in a single nitrogen superhyperfine coupling as is observed. Our ESR results do not entirely exclude these possibilities.

Other Remarks. It may be worthwhile to mention that the hydrogen bonded plane formed between two adjacent cytosine molecules is quite similar to those in the cytosine-guanine and adenine-thymine(uracil) pairs in nucleic acids (see Figure 7). If the Cu^{2+} site in cytosine monohydrate is this type of hydrogen bonded plane, our ESR results might suggest a similar possibility in DNA and RNA.

Acknowledgment. The authors wish to thank Miss Keiko Hattori for her help in a part of the ESR measurements to determine the spin Hamiltonian parameters.

References and Notes

(1) (a) A. Lösche and W. Windsch, *Phys. Status Solidi*, **11**, k55 (1965); (b) W. Windsch and M. Welter, *Z. Naturforsch., Teil A*, **22**, 1 (1967); (c) K. Takeda, Y. Arata, and S. Fujiwara, *J. Chem. Phys.*, **53**, 854 (1970); (d) M. Fujimoto and J. Janecka, *ibid.*, **55**, 1152 (1971); (e) B. A. Wilkinson, Jr., and I. Miyagawa, *ibid.*, **55**, 2177 (1971); (f) M. Fujimoto, L. A. Wylie, and S. Saito, *ibid.*, **58**, 1273 (1973); (g) T. Kato and R. Abe, *J. Phys. Soc. Jpn.*, **35**, 1643 (1973); (h) J. Stankowski and A. Wieckowski, *J. Magn. Reson.*, **15**, 498 (1974).
(2) For example, G. L. Eichorn and P. Chank, *Proc. Nat. Acad. Sci. U.S.A.*, **53**, 586 (1965).
(3) For example, (a) Ch. Zimmer, G. Luck, H. Fritzsche, and H. Triebel, *Biopolymers*, **10**, 441 (1971); (b) H. Richard, J. P. Schreiber, and M. Dane, *ibid.*, **12**, 1 (1973).
(4) G. A. Jefferey and Y. Kinoshita, *Acta Crystallogr.*, **16**, 20 (1963).
(5) M. Iwasaki, *J. Magn. Reson.*, **16**, 417 (1974).
(6) (a) A. H. Maki and B. R. McGarvey, *J. Chem. Phys.*, **29**, 31, 35 (1958); (b) D. Kivelson and R. Neiman, *ibid.*, **35**, 149 (1961); (c) G. Rist, J. Ammeter, and Hs. H. Gunthard, *ibid.*, **49**, 2210 (1968).
(7) A. Kawamori and I. Miyagawa, *J. Chem. Phys.*, **55**, 1336 (1971).